ISSN 2616-7433 Vol. 2, Issue 9: 62-67, DOI: 10.25236/FSST.2020.020914

Enhanced quantum spin pumping in magnetic field effect semiconductor

Yun-Chang Xiao[1], Qiong Mei[2] , Ri-Xing Wang[1]

1 College of Computer and Electrical Engineering, Huas, Changde 415000, China
2 Furong College Hunan University of Arts and Science, Changde 415000, China

ABSTRACT. *Modulations of the quantum spin pumping were investigated in magnetic field effect semiconductors. With Floquet technology, theoretical realizations of the semiconductor pump are shown clear and feasible. Due to perpendicular magnetic fields in a semiconductor with two types of spin-orbit couplings (SOCs), spin polarized pumpings can be produced. Moreover, pure spin currents are enhanced by proper modulations of the magnetic fields and SOCs, and thus a good quantum spin pumping can be realized.*

KEYWORDS: *Semiconductor pump, Perpendicular external fields, Pure spin currents*

1. Introduction

Quantum pumpings (QPs), regardless of whether there is any bias voltage in a system, can be used to realize quantized spin/charge rectifications by variation of the systemic parameters. It was proposed for the first time in atomic chains to generate directed and quantized currents [1]. Similar to classical pumping applications of driving the matter moved in designated directions, for two or even more parameters of the system, a QP will be prominently formed when the cyclic adiabatic changes appear [2-7]. In order to get more significant rectified currents in mesoscopic structures, formations and manipulations of the pumping have been attracted lots of interests [8-11]. Specially, realization of the QP based on semiconductors and driven by time-dependent potentials has been attracted wide investigation interests[12,13], and chronically semiconductor pump manipulated by in helps of ferromagnetic materials has been focused[4].

Usually, oscillated currents of QPs are not only modulated by the driven potentials, but also simultaneously by serial parametric controls such as the magnetic fields and the spin-orbit couplings (SOCs)[14-16]. Manipulations of procession and flipping of the spin electrons can be realized simply, and so far as to an enhanced pure spin pumping in some proper parametric modulations. More actually, formation of the most enhanced pure spin current can be produced by co-effects of the magnetic fields and two SOCs. In order to make sure the physical mechanisms and image interpretations of the most enhanced pure spin pumping, the QP modulations are given in detail in this work.

Rests of the paper are shown as follows: the research model and related theoretical methods are given in Section II; the numerical results are presented in Section III and a brief conclusion is shown in Section IV.

2. Model and Formulation

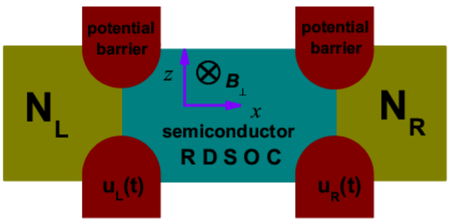

Fig. 1 The two SOCs effect semiconductor pump. There are normal leads in the left and right side, and a semiconductor due to the R-D SOCs and perpendicular magnetic fields in the middle. A double time dependent potential is located between the interfaces.

The suggested model is made up by three different regions, a semiconductor and two normal wires as shown in Fig. 1. Both of the interfaces are placed by double time dependent delta potentials. The left and right regions

ISSN 2616-7433 Vol. 2, Issue 9: 62-67, DOI: 10.25236/FSST.2020.020914

are leads, they are N_α ($\alpha = L, R$ are side of the leads or potentials) and with no SOCs. Here a quasi-one-dimensional quantum wire is suggested to describe the system. While one chooses the electron dynamic direction along x axis, Hamiltonian of the leads can be written as [3,15]

$$\hat{H}_{\text{Lead}}(x,t) = \frac{\hat{p}_x^2}{2m_{\text{f}}} + \sum_\alpha u_\alpha(t)\delta(x'_\alpha), \tag{1}$$

where the driving potentials are included, p_x is the momentum operator and m_{f} is the effective electron mass. Sum part of above Hamiltonian are potentials, where $x'_\alpha = x - x_\alpha$ and x_α marks positions of interfaces, and the semiconductor size is fixed as $\ell = x_R - x_L$. For driven potentials, the static and dynamic potentials are same settings and they are expressed as $u_\alpha(t) = u_{\alpha s} + u_{\alpha d}\cos(\omega t + \varphi_\alpha)$, with ω an oscillation frequency and $\varphi = \varphi_R - \varphi_L$ a phase difference. Due to a perpendicular magnetic field, Hamiltonian of the middle region is[15]

$$\hat{H}_{\text{soc}}(x) = \frac{\hat{p}_x^2}{2m_{\text{s}}} - \frac{\hbar k_{\text{so}}}{m_{\text{s}}}\hat{\sigma}_{\text{so}}\hat{p}_x + \hat{B}_\perp \sigma_y. \tag{2}$$

Here m_{s} denotes the effective electron mass in a semiconductor, k_α / k_β are corresponding to the Rashba/Dresselhaus SOCs, they construct a combined SOC wave-vector $k_{\text{so}} = \sqrt{k_\alpha^2 + k_\beta^2}$ and $\sin\theta = k_\beta / k_{\text{so}}, \cos\theta = -k_\alpha / k_{\text{so}}$. Consequently, spin operator of the combined SOCs can be recorded as $\hat{\sigma}_{\text{so}} = \hat{\sigma}_x \sin\theta + \hat{\sigma}_z \cos\theta$ ($\sigma_{i=x,y,z}$ are Pauli matrix). As affected by magnetic fields $B_\perp$, which is perpendicular to spin-movement plane of the electron transport, the wave vector can be get as $k_\perp = \sqrt{2m_{\text{s}}B_\perp} / \hbar$.

The time dependent driven potentials can be made up by series position wave functions, and thus the Floquet-eigenstates are $\Psi_\alpha^\varepsilon(x,t) = \sum_{n=-\infty}^{\infty} \psi_\alpha^n(x) e^{-i\omega_n t}$. Where $\omega_n = (\varepsilon + n\hbar\omega)/\hbar$ is the oscillation frequency of the *n*th propagating mode, ε is an insert energy and $\hbar\omega$ is an energy quantum. With spin operation of the two normal leads, the electron spinors are $\sigma_\alpha = \sigma = \uparrow, \downarrow$, which is equated to $|+\rangle = (1,0)^\dagger, |-\rangle = (0,1)^\dagger$ with $\hat{\sigma}_z|\sigma\rangle = \pm|\sigma\rangle$. In *x* direction, electron forwarding in the *n*th propagating mode of the normal leads general has expressions as

$$\psi_\alpha^n(x) = \sum_\sigma \left(a_{\alpha n}^\sigma e^{\eta i k_n x'_\alpha} + b_{\alpha n}^\sigma e^{-\eta i k_n x'_\alpha} \right) |\sigma\rangle, \quad \eta x'_\alpha \le 0. \tag{3}$$

Where $\eta = (-1)^\nu$ is a location factor and decided by the side difference of $\nu = \delta_{\alpha R}$, $a_{\alpha n}^\sigma, b_{\alpha n}^\sigma$ indicate the incoming and outgoing amplitudes and $k_n = \sqrt{2m_{\text{s}}\omega_n / \hbar}$ are wave vectors. In *n*th eigenstate of the central region of $x \in [x_L, x_R]$, the electron wave functions are made by linear combination of the momentum and the spin operator

$$\psi_S^n(x) = \sum_{j=1}^{4} c_{nj} \left(\chi_{nj}^\uparrow, \chi_{nj}^\downarrow \right)^\dagger e^{ik_{nj}x'_L}. \tag{4}$$

ISSN 2616-7433 Vol. 2, Issue 9: 62-67, DOI: 10.25236/FSST.2020.020914

Where c_{nj} are parameters to be determined and $\chi_{nj}^{\uparrow} = k_{\beta} k_{nj} + ik_{ex}$, $\chi_{nj}^{\downarrow} = \frac{1}{2}\left(k_{nj}^2 - \tau k_n^2\right) + k_{\alpha} k_{nj}$, $\tau = m_{\mathrm{s}} / m_{\mathrm{f}}$ means the effective mass difference of vary regions and k_{nj} are wave vectors derived from eigen-equations.

In propagating modes, wave functions ψ_{α}^{n} and ψ_{S}^{n}, which are belong to regional Floquet eigenstates, can be resolved by continuity conditions including the wave functions and current conservations[15,16]. By taking into account wave functions to the continuity conditions, pumping properties can be solved by the Floquet scattering matrices

$$U_n X_{\alpha nj}^{\sigma} + 2\tau X_{\alpha 0}^{\sigma} = D_{n+1} X_{\alpha(n+1)j}^{\sigma} + I_{n-1} X_{\alpha(n-1)j}^{\sigma}. \quad (5)$$

The parametric matrix $X_{\alpha nj}^{\sigma} = (\chi_{Lnj}, \quad \chi_{Rnj})^T$ with $\chi_{\alpha nj} = c_{nj} \chi_{nj} e^{ik_{nj}\ell\delta_{\alpha R}}$, where spin components are simply written as $\chi_{nj} = (\chi_{nj}^{\uparrow}, \quad \chi_{nj}^{\downarrow})^T$, can be got from Eq. (4). The incoming matrix $X_{\alpha 0}^{\sigma} = \delta_{0n}(\chi_L, \quad \chi_R)^T$ can establish a matrix relation of different propagating modes. Indices of U_n, D_{n+1}, I_{n-1} are derived from

$$\begin{aligned} &\sum_j \left(\gamma_{\alpha nj}\chi_{\alpha nj}^{\sigma} - \gamma_{\alpha n\beta}\chi_{\alpha nj}^{\bar{\sigma}}\right) - 2\tau\chi_{\alpha 0}^{\sigma} \\ &= -h_{dn}\left[e^{i\varphi_\alpha}\sum_j \chi_{\alpha(n+1)j}^{\sigma} + e^{-i\varphi_\alpha}\sum_j \chi_{\alpha(n-1)j}^{\sigma}\right]. \end{aligned} \quad (6)$$

Where the matrix elements details are $\chi_{\alpha nj}^{\sigma} = c_{nj}\chi_{nj}^{\sigma} e^{ik_{nj}\ell\delta_{\alpha R}}$ and $\chi_{\alpha 0}^{\sigma} = \delta_{0n}\delta_{\alpha'\alpha}\delta_{\sigma'\sigma}$ with $\bar{\sigma}$ the opposite spin of σ, the potential parameters are $h_{\zeta n} = \frac{m_{\mathrm{s}} u_{\zeta}}{\hbar^2 k_n}$ with $\zeta = s, d$, and $\gamma_{\alpha nj} = \tau + h_{sn} + \eta k_{nj} / k_n, \gamma_{\alpha n\beta} = \eta k_{\mathrm{so}} / k_n$.

As involving expressions of the lead spin indices $\sigma_{\alpha}, \sigma_{\alpha}'$ ($\alpha, \bar{\alpha}$ mean opposite leads of each other), the reflection and transmission coefficients can be written as $r_{\alpha n}^{\sigma_{\alpha}'\sigma_{\alpha}}$ and $t_{\alpha n}^{\sigma_{\bar{\alpha}}'\sigma_{\alpha}}$. Which is derived from Floquet scattering matrix of spin elements $b_{\alpha n}^{\sigma_{\alpha}} = T_{\alpha n}^{\sigma_{\alpha}\sigma_{\alpha}'} a_{\alpha n}^{\sigma_{\alpha}}$, and where $T_{\alpha n}^{\sigma_{\alpha}\sigma_{\alpha}'} = \left(r_{Ln}^{\sigma_L\sigma_L'}, t_{Rn}^{\sigma_L\sigma_R'}; t_{Ln}^{\sigma_R\sigma_L'}, r_{Rn}^{\sigma_R\sigma_R'}\right)^{\dagger}$ is the scattering matrix related to amplitudes of the outgoing $\left\{b_{\alpha n}^{\sigma_{\alpha}}\right\}$ and the incoming $\{a_{\alpha n}^{\sigma_{\alpha}'}\}$ .In the pumping procedure, an adiabatic current flowing can be derived from the transmission coefficients. For any leads α , the pumping currents have expressions as $I_{\alpha}^{\sigma} = \frac{e\omega}{2\pi}\sum_n n\left(\left|t_{\bar{\alpha}n}^{\sigma_{\alpha}\sigma_{\bar{\alpha}}'}\right|^2 - \left|t_{\alpha n}^{\sigma_{\bar{\alpha}}\sigma_{\alpha}'}\right|^2\right)$ and all propagating modes make effects to the current flowing. In α lead, the pumped charges are $I_{\mathrm{c}} = I_{\alpha}^{\uparrow} + I_{\alpha}^{\downarrow}$, where the spin up and spin down sub-bands are both take into account. While for $I_{\mathrm{s}} = I_{\alpha}^{\uparrow} - I_{\alpha}^{\downarrow}$, which means that the spin currents depend on the electrons of spin up but subtract the spin down.

3. Numerical Results and Discussions

Throughout the letter, the SOCs are realized in a typical InAs-based semiconductor and $\tau = 0.053$ represents the mass difference of vary regions[3,15,16]. Size of the device is chosen as $\ell = 100nm$, the insert energy is $\varepsilon = 0.3\mathrm{eV}$ and one percent of which is an energy quantum $\hbar\omega$. Furthermore, a controlled energy wave $\kappa_0 = 0.01k_0$ corresponds to the energy wave vector $k_0 = 3nm^{-1}$, and driving potentials of the static/ac

ISSN 2616-7433 Vol. 2, Issue 9: 62-67, DOI: 10.25236/FSST.2020.020914

properties are set as $u_d = 3u_s = 0.2\varepsilon$. In this scheme, the right lead is applied to all charge and spin currents, which have the representations of I_c and I_s. All over the calculations, the phase differences of the potentials are always fixed as $\varphi = \pi / 2$, and in order to get a more straightforward picture of the pure spin pumpings, the assisted dash-dot-dot lines are added in following figures..

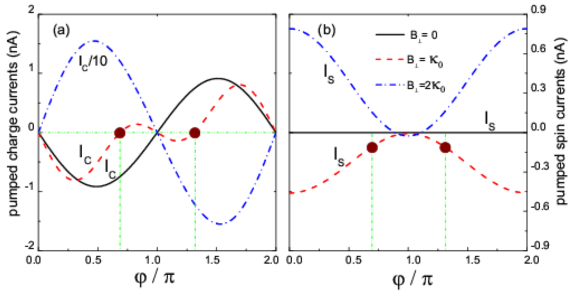

Fig. 2 Pumping properties versus phase differences in vary perpendicular magnetic fields. Strength of the R-D SOC is chosen as $k_{so} = 5\kappa_0, \theta_{so} = 143^\circ$, and the currents are plotted with vary lines in two panels corresponding to the charges and spins.

Modulations of the pumped current driven by phase differences are shown in Fig. 2. In this situation, the pumping is subjected to a settled R-D SOCs ($k_{so} = 5\kappa_0, \theta_{so} = 0.79\pi$ are corresponding to $3k_\alpha = 4k_\beta = 12\kappa_0$) with vary perpendicular magnetic fields. For solid lines of $B_\perp = 0$, which mean that there are no magnetic fields along the semiconductor, and the whole pumping is only subjected to two SOCs. The lines show that anti-sinusoidal charge currents without spin currents appear in this clean system (as shown by the two panels of Fig. 2). Addition of the magnetic fields makes different modulations to the charge current, as shown by the dashed lines of $B_\perp = \kappa_0$. Oscillations of the current are still keeping same amplitudes but the periods are increased, and thus the spin currents are pumped. Meanwhile, the charge currents are larger than the spins. This result makes the spin pumping is hard to be enhanced, but the phase difference can produce many pure spin currents, as shown by the right panel of Fig. 2. Generally, the figure reveals that increasing of the perpendicular magnetic fields induces the systematic time reversal broken heavily, and modulations of the spin/charge currents are strengthen [15].

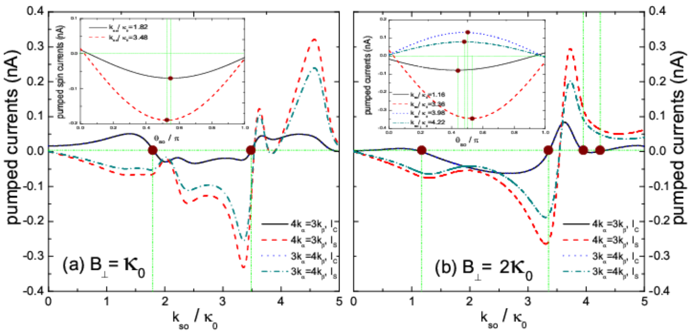

Fig. 3 Current pumpings as a function of combined SOC strength. The solid, dotted lines are pumping of charges and the rests are pumping of spins. Production of enhanced pure spin current pumpings can be achieved by proper adjustments to the SOC component.

Usually, spin polarizations of the system are greatly modulated by the SOC strengths and components in different magnetic fields. Therefore, Fig. 3 shows that spin currents present significant oscillations with the SOCs. The figures also show that in every settled SOC component and magnetic field, tunings of proper SOC strengths can obtain an enhanced pure spin current. Physical mechanism of the phenomenon mainly comes from that in the R-D system, the perpendicular magnetic field makes the spins oscillate with large contrary phases. Furthermore, a stronger magnetic field imposed, an easier pumping can be realized to the charges and the spins, the phenomena can be seen in Fig. 3(b). Comparing with the charges and spins of the panels, one can get that there are even more smoothly and stronger oscillations of the spins, and they make the pure spin currents changed. For specific performance four pure spin current pumping in different SOC strengths are shown. Increasing the D SOC strength, and referred the assisted points in the left-up panel of Fig. 3(b), a larger SOC strength makes the spin pumping oscillation peaks increase to the two negative oscillation peaks, and the pure spin currents can even achieve some positive values. This induces a method of producing an extremely enhanced pure spin currents pumping. The results come from that in large magnetic fields increasing proper R-D SOC strengths makes spin pumping of the semiconductor much more precise and significant.

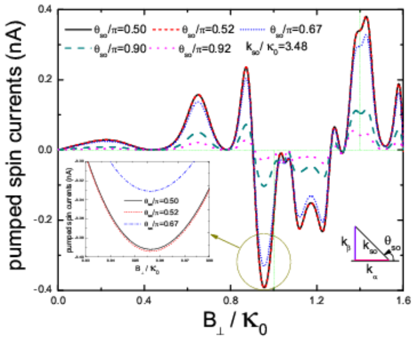

Fig. 4 The spin current pumping as a function of the perpendicular magnetic fields in settled SOC strength. With proper modulations of the SOC components, an increased pure spin current can be achieved. The most enhanced pure spin current pumping can be seen in the left-down panel, and the right-down panel is the relationship of the R-D SOCs.

Moreover, magnetic field effect to the semiconductor bulks is always investigated by its prominent modulations to the electron charges and spins. It is important to reveal dramatic influence of the magnetic fields to quantum pumpings in semiconductors, extremely involve the spin currents pumping. In Fig. 4, the spin pumpings are plotted with vary perpendicular magnetic fields in different SOC types. Compared both of the amplitudes and periods of the spin currents, the magnetic fields induced oscillations are always large and quick. This easily leads to a pure spin current pumping. Moreover, for settled SOC couplings and magnetic fields, a pure spin current can be enhanced by variation of the SOC component. All these spin currents are produced by a settled SOC strength, which makes there are no any charge pumping in proper perpendicular magnetic fields, thus a pure spin current can be produced. Furthermore, in this condition, varying of the SOC components can change the spin current pumping, thus one can make the most enhanced pure spin current, it is present by the left dash-dotted line added in the figure. One can also see that oscillations of the spin current pumpings are large increased in amplitude as the D SOC component strengthened. Actually, the largest oscillation amplitude is not appear in the whole D SOC component, but in a coexist of a large D SOC with a small R SOC, i.e., $\theta_{so} = 0.52\pi$, which means that as influenced by the magnetic fields, electron spin oscillations in the semiconductor will be adjusted by two types SOCs with different amplitude and phase.

5. Conclusion

In summary, descriptions and discussions of the pumped currents modulated by vary perpendicular magnetic fields in semiconductors are present. Pure spin currents can be obviously modulated by the magnetic fields, and the SOCs in both of the strength and component properties. As easily modulated by some perpendicular magnetic fields, a good spin pumping modulation can be significant enhanced by component tunings of the SOCs. The results are meaningful for design of the specific quantum pumping devices, especially for realizations of the spin pumping devices. We thank the support from the Major Scientific Research Fund of Hunan University of Arts and Science (Grant No. 16ZD04) and the Scientific Research Foundation of Education Bureau of Hunan Province (Grant No.17C1080).

Acknowledgment

Major Scientific Research Fund of HUAS (Grant No. 16ZD04) and the Scientific Research Foundation of Education Bureau of Hunan Province (Grant No.17C1080).

References

[1] Thouless D J (1983). Quantization of particle transport. Phys Rev B, no.27, pp.6083.
[2] Brouwer P W (1998). Scattering approach to parametric pumping. Phys Rev B, no.58, pp. R10135
[3] Moskalets M, Buttiker M (2002). Floquet scattering theory of quantum pumps. Phys Rev B, no.66, pp.205320.

ISSN 2616-7433 Vol. 2, Issue 9: 62-67, DOI: 10.25236/FSST.2020.020914

[4] Watson S K, et al (2003). Experimental Realization of a Quantum Spin Pump. Phys Rev Lett, no.91, pp.258301
[5] Strass M, HÄanggi P, Kohler S (2005). Nonadiabatic Electron Pumping: Maximal Current with Minimal Noise. Phys. Rev. Lett, no.95, pp.130601.
[6] Avishai Y, et al (2010). Purely Electric Spin Pumping in One Dimension. Phys Rev Lett, no.104, pp.196601.
[7] Russomanno A., et al (2011). Floquet theory of Cooper pair pumping. Phys Rev B, no.83, pp.214508
[8] Faizabadi E (2007). Charge and spin pumping in quantum wires by a time-dependent periodic magnetic field. Phys Rev B, no.76, pp.075307.
[9] Splettstoesser J, Governale M, KÄonig J (2008). Adiabatic charge and spin pumping through quantum dots with ferromagnetic leads. Phys Rev B, no.77, pp.195320.
[10] Nakajima S, et al (2016). Topological thouless pumping of ultracold fermions. Nature Phys, no.12, pp.296.
[11] Korniyenko Y, Shevtsov O,et al (2017). Shot noise in a harmonically driven ballistic graphene transistor. Phys Rev B, no.95, pp.165420
[12] Cahay M, Bandyopadhyay S (2003). Conductance modulation of spin interferometers. Phy Rev B.
[13] Mal'shukov A G, Tang C S, Chu C S, et al (2003). Spin-current generation and detection in the presence of an ac gate.Phys Rev B.
[14] Schliemann J, Egues J C and Loss D (2003). Nonballistic Spin-Field-Effect Transistor.Phys Rev Lett, no.90, pp.146801
[15] Xiao Y C, et el (2016). Quantum pump in a system with both Rashba and Dresselhaus spin–orbit couplings. Phys Lett A, 2013, 377:817; Xiao Y C, et al. Arbitrary magnetic field modulations to a semiconductor pump with two types of spin-orbit couplings. J. Senicond, no.37, pp.014009.
[16] Benjamin R and Benjamin C (2004). Quantum spin pumping with adiabatically modulated magnetic barriers. Phys Rev B, pp.69-70.